(2) E. A. Kiamco and E. Hellmuth, Abstracts, 5th International Conference on Liquid Crystals, Stockholm, June 1974; *Bull. Am. Phys. Soc.*, **20**, 313 (1975).
(3) A. Blumstein, R. Blumstein, S. Clough, and E. Hsu, *Macromolecules* **8**, 73 (1975).
(4) A. Blumstein, paper presented at 3rd Midland Macromolecular Meeting, August 1974, to be published in *Int. J. Polym. Sci.*
(5) C. Paleos, T. Larange, and M. Labes, *Chem. Commun.*, 1115 (1968).
(6) C. Paleos and M. Labes, *Mol. Cryst. Liq. Cryst.*, **11**, 385 (1970).
(7) E. Perplies, H. Ringsdorf, and J. Wendorff, *Makromol. Chem.*, **175**, 553 (1974).
(8) E. Perplies, H. Ringsdorf, and J. Wendorff, *J. Polym. Sci., Polym. Lett.*, **13**, 243 (1975).
(9) L. Liebert and L. Strzelecki, *Bull. Soc. Chim. Fr.*, 597 (1973); 603 (1973).
(10) L. Liebert and L. Strzelecki, *C. R. Hebd. Seances Acad. Sci.*, **276**, 647 (1973).
(11) Y. Bouligand, P. Cladis, L. Liebert, and L. Strzelecki, *Mol. Cryst. Liq. Cryst.*, **25**, 233 (1974).
(12) B. A. Newman, V. Frosini, and L. Magagnini, *J. Polym. Sci., Polym. Phys. Ed.*, **13**, 87 (1975).
(13) A. deVries, *Mol. Cryst. Liq. Cryst.*, **10**, 31 (1974).
(14) E. Hsu, L. Lim, R. Blumstein, and A. Blumstein, *Mol. Cryst. Liq. Cryst.*, submitted for publication.
(15) N. A. Platé and V. P. Shibaev, *J. Polym. Sci., Macromol. Rev.*, **8**, 117 (1974).
(16) A. deVries, *Mol. Cryst. Liq. Cryst.*, **20**, 119 (1973).
(17) O. G. Lewis, "Physical Constants of Linear Homopolymers", Springer-Verlag, New York, N.Y., 1968.
(18) G. Brown, J. Doane, and V. Neff, "A Review of the Structure and Physical Properties of Liquid Crystals", Chemical Rubber Publishing Co., Cleveland, Ohio, 1971, p 19.
(19) E. C. Hsu, to be published.
(20) A. deVries, *Mol. Cryst. Liq. Cryst.*, **10**, 219 (1970).
(21) P. Parikh, M.S. Thesis submitted to Department of Plastics, University of Lowell, July, 1975.

Rheological Properties of Linear and Branched Polyisoprene

W. W. Graessley,*[1a] T. Masuda,[1a] J. E. L. Roovers,[1b] and N. Hadjichristidis[1b,c]

Chemical Engineering and Materials Science Departments, Northwestern University, Evanston, Illinois 60201, and Division of Chemistry, National Research Council of Canada, Ottawa, Canada KIA OR9. *Received October 7, 1975*

ABSTRACT: Viscosity η and first normal stress N_1 have been measured as functions of shear rate $\dot{\gamma}$ for solutions of linear, four-arm star, and six-arm star polyisoprenes, all with narrow molecular weight distributions. Concentrations in tetradecane ranged from 0.02 g/ml to 0.33 g/ml; molecular weights ranged from 35 000 to 2 000 000. All measurements were made at 25 °C in a Weissenberg Rheogoniometer. The effects of branching on zero shear viscosity η_0, steady state compliance J_e^0, the characteristic shear rate (marking the onset of shear rate dependence in η) $\dot{\gamma}_0$, and the shape of the η vs. $\dot{\gamma}$ master curve were determined. At low concentrations and molecular weights the values of η_0 and J_e^0 were lower for the branched samples, while at high concentrations and molecular weights the reverse became true and substantial enhancements in η_0 and J_e^0 were found. On the other hand, the product $\eta_0 J_e^0 \dot{\gamma}_0$ was essentially the same for all samples irrespective of concentration, molecular weight, or branching, and the form of the master curve appeared to be independent of branching. Enhancement factors were determined and compared with results reported by Kraus and Gruver on star-branched polybutadienes. Data on viscosity enhancement for the two polymers reduced to essentially the same curve when correlated in terms of $\Phi^{5/6}(\Phi M_b/M_c)$, Φ being the volume fraction of polymer, M_b the molecular weight of the branches, and M_c the characteristic molecular weight for entanglement in the respective undiluted linear polymers. The form of this correlating parameter was arrived at by considerations on the effect of long branches on macromolecular mobility in entangling systems. The interpretation of enhancement in η_0 and J_e^0 in relation to the spectrum of relaxation times and their practical effects on η vs. $\dot{\gamma}$ behavior are discussed.

I. Introduction

The flow properties of polymers are altered by branching in important and unexpected ways.[2-8] Quantitative information on the relationship between branch structure and behavior is still scanty, however, and molecular explanations for the observations are almost totally lacking. This paper presents some results obtained in steady shearing flow on star-branched polyisoprenes, all of narrow molecular weight distribution and all well characterized by dilution solution methods.[9] It also contains some preliminary attempts to unify the observations with those published for other branched polymers.

Three series of polyisoprene samples were studied: linear molecules, star molecules with four equal arms, and stars with six equal arms. Solutions in tetradecane encompassing a range of polymer concentration c and molecular weight M were prepared with each series. Shear stress σ and first normal stress difference N_1 were measured at 25.5 °C as functions of shear rate $\dot{\gamma}$ in a plate-cone rheometer. Values of the viscosity at zero shear rate η_0, the steady state recoverable compliance J_e^0 (estimated from N_1 at low shear rates), and the characteristic shear rate $\dot{\gamma}_0$ (locating the onset of shear rate dependence in the viscosity) were determined and correlated with structure.

II. Theoretical Background

A. Zero Shear Viscosity. The effects of branching are best established for the case of the zero shear viscosity η_0. When the branches are not too long or when the polymer concentration is sufficiently low, η_0 is less than that for linear chains of the same total molecular weight, presumably due to the smaller mean radius of gyration S of branched molecules. On the other hand, for long branches at high polymer concentrations the viscosity becomes larger in branched systems.

Berry and Fox[2a] discuss the viscosity behavior relative to linear systems in terms of two factors. One governs the reduction, which is assumed to depend only on the ratio of radii and to operate at all concentrations and branch lengths. The other governs enhancement and becomes important, then dominating, at high concentrations and branch lengths. They note that, when the reduction factor alone is acting, the viscosity of branched polymers is approximately the same as for linear polymers of the same ra-

dius of gyration. Thus, the molecular weight dependence of viscosity can in principle be expressed as the same function of S, or some property which depends on S, for both linear and branched chains.

$$\eta_0 = \eta_0(S, c, T, \ldots) \tag{1}$$

The viscosity enhancement factor Γ_1 is then defined in terms of the observed viscosity

$$\Gamma_1 = (\eta_0)_{\text{obsd}}/(\eta_0)_{\text{calcd}} \tag{2}$$

in which $(\eta_0)_{\text{calcd}}$ is obtained from eq 1 or its equivalent. Experimental evaluation of the enhancement factor Γ_1 therefore requires the establishment of a viscosity correlation for linear chains and the application of some relationship for obtaining values of $(\eta_0)_{\text{calcd}}$ which appropriately reflects the smaller radius of branched chains.

The molecular weight dependence of viscosity in linear polymers depends upon the range of concentrations covered.[10] The solutions used in the present study range from $c = 0.03$ g/ml to $c = 0.33$ g/ml and thus extend into both the low and high concentration regimes. At low and moderate concentrations, η_0 for linear polymer systems can be expressed, at least approximately, in terms of a combined dimensionless variable $c[\eta]$. The intrinsic viscosity $[\eta]$ is that measured in the solvent used to make the solutions.

$$\eta_0 = F(c[\eta]) \qquad (\eta_0 \gg \text{solvent viscosity } \eta_s) \tag{3}$$

The product $c[\eta]$ is a measure of the average number of polymer molecules whose centers lie within the pervaded volume of any selected molecule in the system. To the extent that coil overlap alone governs viscosity in the absence of enhancement, branched polymers might be expected to obey the same η_0 vs. $c[\eta]$ correlation as linear polymers.

At high concentrations and molecular weights the viscosity of linear polymers at constant temperature is usually correlated in terms of the combined parameter cM and a concentration-dependent friction coefficient $\zeta_0(c)$:[2a,10,11]

$$\eta_0 = K_1\zeta_0(c)(cM)^a \tag{4}$$

The exponent a is approximately 3.5 when cM exceeds a characteristic value ρM_c. The characteristic molecular weight M_c is 10 000 for polyisoprene,[10] and the polymer density ρ is 0.913 g/ml at 25 °C.[12] For most solutions in this study $cM > 10^4$, so the above form would be expected to apply. Guided by molecular theories of viscosity in free-draining systems,[13,14] Berry and Fox have recast this expression in terms of molecular radius, such that

$$\eta_0 = K_2\zeta_0(c)(cS_\theta^2)^a \tag{5}$$

and S_θ^2 is the unperturbed mean-square radius for either linear or branched chains. In the absence of enhancement, the equation governing both linear and branched polymers can thus be expressed

$$\eta_0 = K_3\zeta_0(c)(cgM)^a \tag{6}$$

in which g is the ratio S_B^2/S_L^2 for branched and linear chains of the same molecular weight. Alternatively,

$$\eta_0 = K_4\zeta_0(c)(c[\eta]_\theta^2)^a \tag{7}$$

if the approximate Zimm–Kilb relationship:[15]

$$[\eta]_B/[\eta]_L = g^{1/2} \tag{8}$$

and the relationship for linear random coils in theta solvents, $[\eta]_\theta \propto M^{1/2}$, are applied.

Equations 3, 6, and 7 will be used to evaluate enhancement factors for the star-branched polymers in this work. The theoretical expression for g in random coil, equal arm, f-star molecules is[13]

$$g = (3f - 2)/f^2 \tag{9}$$

B. Steady-State Recoverable Compliance. Experience with branched polymers is much more limited in the case of recoverable compliance J_e^0. The Rouse theory,[16] as extended by Ham[13] to the case of f-arm star molecules, yields

$$J_e^0 = \frac{2}{5}g_2\frac{M}{cRT} \qquad (\eta_0 \gg \eta_s) \tag{10}$$

in which

$$g_2 = (15f - 14)/(3f - 2)^2 \tag{11}$$

This and similar calculations for other types of branched structures predict compliances which are less than those for linear polymers of the same molecular weight. Experimental behavior near the limit of zero concentration[17] as well as some data at higher concentrations[6,8] are consistent with such calculations, but other results in concentrated solutions and melts show compliances in branched polymers which are higher than corresponding linear polymers by a factor of 10 or more.[3,5]

Data on several linear polymers of narrow molecular weight distribution have been correlated[10] according to the following approximate form (for $\eta_0 \gg \eta_s$):

$$J_e^0 = \alpha\frac{M}{cRT} \qquad cM < \rho M_c' \tag{12}$$

$$J_e^0 = \alpha\frac{M}{cRT}\left(\frac{\rho M_c'}{cM}\right) \qquad cM > \rho M_c' \tag{13}$$

in which α is a constant approximately equal to the Rouse theory value of 0.4, and M_c' is a characteristic molecular weight with a value of approximately 60 000 for linear polyisoprene.[10]

It is not clear how to modify these equations to reflect the reduction of compliance due to branching at low concentrations and branch lengths, and thus provide a means for calculating an enhancement factor for compliance Γ_2 from experimental data at high concentrations. One possible procedure, somewhat arbitrary but analogous to the analysis of viscosity enhancement, is to estimate the compliance in the absence of enhancement from

$$J_e^0 = 0.4g_2\frac{M}{cRT} \qquad cgM < \rho M_c' \tag{14}$$

$$J_e^0 = 0.4\frac{g_2M}{cRT}\left(\frac{\rho M_c'}{cgM}\right) \qquad cgM > \rho M_c' \tag{15}$$

The compliance factor is then given by

$$\Gamma_2 = (J_e^0)_{\text{obsd}}/(J_e^0)_{\text{calcd}} \tag{16}$$

in which $(J_e^0)_{\text{calcd}}$ is obtained from eq 14 and 15 (or their equivalent if some other behavior were found for linear polymers). Unless g_2 can be evaluated independently, theoretical expressions such as eq 11 must be used.

C. Characteristic Shear Rate. The shear rate dependence of viscosity can be expressed in reduced form[10]

$$\eta/\eta_0 = V(\dot\gamma/\dot\gamma_0) \tag{17}$$

The form of the master function V in concentrated systems of linear polymers depends principally on molecular weight distribution. The characteristic shear rate $\dot\gamma_0$ locates the onset of shear rate dependence in $\eta(\dot\gamma)$, and can be chosen in a number of roughly equivalent ways. Several years ago Leaderman[18] noted that $1/\dot\gamma_0$ was proportional to a product of linear viscoelastic parameters, $\eta_0J_e^0$, the precise value of the proportionality constant depending on how $\dot\gamma_0$ was defined. If $\dot\gamma_0$ is taken as the shear rate at which η has fallen

Table I
Summary of Molecular Characterization Data

Sample	$\bar{M}_n \times 10^{-3}$	$\bar{M}_w \times 10^{-3}$	$[\eta]$, dl/g Dioxane (34 °C)	Toluene (34 °C)	Tetradecane (25.5 °C)[a]
H5P	19.9	25.7	0.197	0.312	0.223
H2P	78	83	0.374	0.766	0.489
Pl	105	115	0.448	0.969	0.602
S8P	209	240	0.630	1.66	0.967
P5	358	394	0.835	2.35	1.395
P3		591	1.02	3.21	1.845
P4		1611	1.70	6.90	(3.65)
P2		2225	1.97	8.48	(4.55)
S4	35.2	37.8	0.193	0.316	(0.214)
S7	66.9	67.1	0.266	0.477	(0.312)
S2	101.2	107.6	0.326	0.665	(0.437)
S1	195	215	0.476	1.112	(0.69)
S3	432	449	0.677	1.855	(1.13)
S8		880	0.945	3.27	(1.80)
S6		1950	1.47	5.70	(3.08)
H7	43.6	45.4	0.177	0.294	(0.194)
H6	83.5	85.7	0.242	0.450	(0.298)
H5	117	122	0.288	0.588	(0.380)
H1	223	226	0.393	0.915	(0.570)
H2	462	478	0.565	1.60	(0.955)
H4		870	0.765	2.56	(1.425)
H3		1446	0.995	3.81	(2.02)

[a] Values of intrinsic viscosity in tetradecane were measured on several samples. The values in parentheses were calculated as described in the text.

to $0.8\eta_0$, the data on several linear, narrow distribution polymers over a very wide range of concentrations, temperatures, and molecular weights can be expressed as[10]

$$\dot{\gamma}_0\eta_0 J_e^0 = 0.6 \pm 0.2 \qquad (\eta_0 \gg \eta_s) \tag{18}$$

Since only rheological parameters appear, one might anticipate that the same value for this dimensionless group would apply to branched polymers also. If so, enhanced values of both J_e^0 and η_0 should produce an unusually early onset of shear rate dependence in branched polymers. Such behavior has been observed[19] but quantitative tests of eq 18 for branched polymers have not been reported.

Procedures. Molecular characteristics of the samples used in this study[9] are given in Table I. In addition, values of $[\eta]$ in tetradecane were measured for several of the linear samples. Values listed for the remaining polymers are interpolations based on earlier reported data in other solvents.

Solutions of approximately 40 wt % polymer were prepared by combining weighed amounts of polymer and tetradecane (Phillips pure grade, bp 254 °C, $\rho_s = 0.753$ g/ml, and $\eta_s = 0.0206$ P at 25.5 °C) containing 0.02% ionol with an excess of pentane (Fisher practical grade, bp 33–36 °C) at room temperature. With periodic stirring a uniform solution was obtained after 1 day. The pentane was then evaporated at room temperature for 3 or 4 days, and the remainder stripped off under vacuum. Final concentrations in tetradecane were converted to grams per milliliter at 25 °C using densities of the pure components and an assumed additivity of volumes. Samples of lower concentration were made by dilution. Comparison of GPC traces before and after dissolution, and also after the subsequent rheological studies, showed no change in the molecular structure of the polymer. Preliminary studies had shown that heating to 70 °C under vacuum to hasten removal of pentane did indeed produce changes in the GPC trace. The samples used here were never heated above 30 °C.

Rheological measurements were made at 25.5 °C in a Weissenberg Rheogoniometer (Model R-16), modified by replacing the normal force spring and transducer by a rigidly mounted piezo-electric (quartz) crystal and charge amplifier. Occasionally the torque was measured by a similar device, but usually the conventional torsion bar system was used. The crystals and torsion bars (D = ¼ and ⅛ in.) were calibrated statically over the entire range of normal thrusts and torques used in this study. Nearly all measurements were made with a 2° gap angle and 5-cm diameter cone. For the most viscous samples however, a 4° gap angle and 2.5-cm diameter cone was used. Readings were converted to shear stress σ, first normal stress difference N_1, and shear rate $\dot{\gamma}$ with the standard equations for the plate-cone geometry. Examples of data obtained are shown in Figures 1–5.

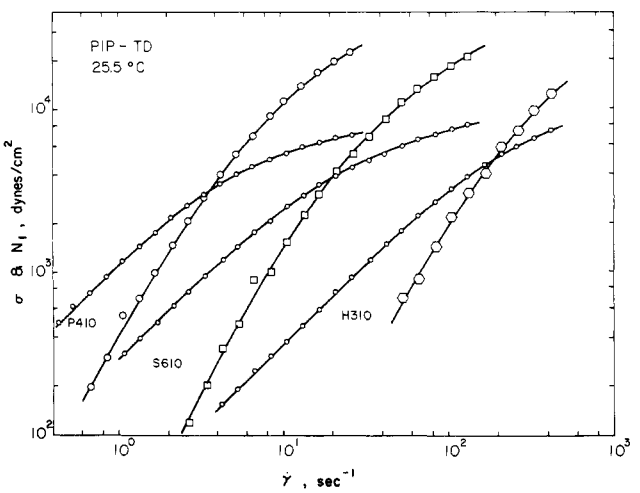

Figure 1. Shear stress and first normal stress data for 10% solutions of polyisoprene. Shear stress is indicated by small circles in each case. Normal stress is indicated by large symbols: linear P410 (○), four-arm star S610 (□), and six-arm star H310 (⬡).

Measurements of molecular weight dependence were made at a concentration of 0.33 g/ml for linear, four-star, and six-star samples. Measurements of concentration de-

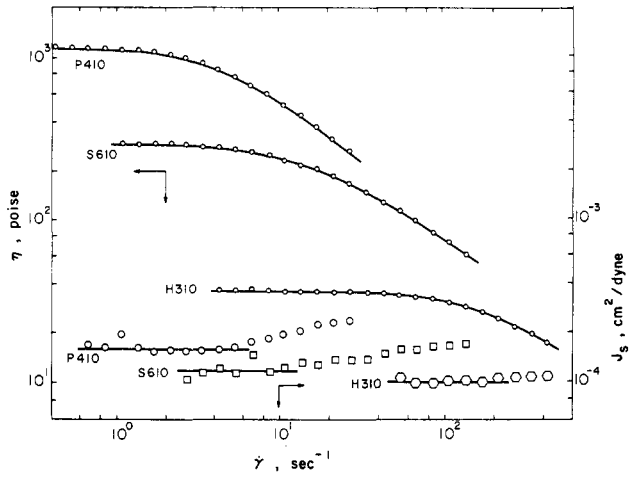

Figure 2. Viscosity η and normal stress compliance J_s as functions of shear rate for 10% polyisoprene solutions. Symbols have the same meaning as in Figure 1.

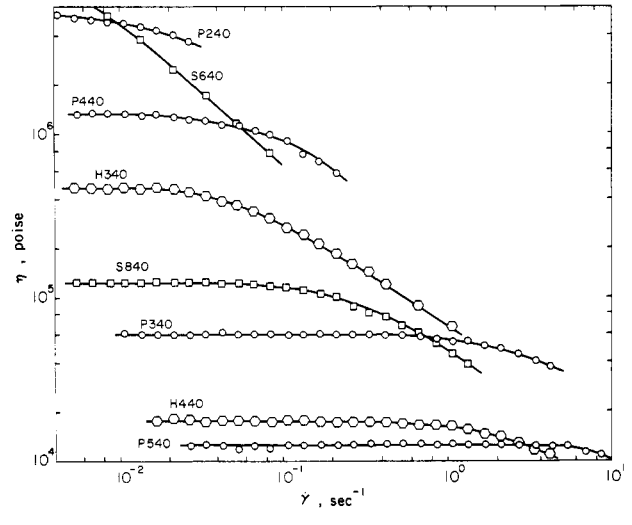

Figure 3. Viscosity vs. shear rate behavior for solutions of various polyisoprenes.

pendence were made for one high molecular weight sample from each group by successive dilution from c = 0.33 g/ml to approximately c = 0.02 g/ml. In all samples but one (S640) it was possible to reach the Newtonian region at low shear rates and thus to determine η_0. The upper limit of shear rate for each sample was set as usual by the development of a flow instability with consequent exudation of sample from the plate-cone gap. The presence of the instability became evident visually through the development of irregularities at the gap edge and also by a slow downward drift of the shear stress reading. As in earlier studies with other polymers,[20-22] the appearance of the instability corresponds in a rough way to the onset of shear rate dependence in the viscosity, with more or less systematic variations with molecular weight and concentration. The behavior was such that a reasonable penetration into the shear-dependent region was possible for high molecular weight polymers at low to moderate concentrations, while practically no penetration was possible for low molecular weight samples at high concentrations. No special difference in this regard was noted between linear and branched samples.

The characteristic shear rate $\dot{\gamma}_0$ was chosen as the shear rate at which the viscosity has fallen to 80% of its zero shear value (η/η_0 = 0.8 at $\dot{\gamma}_0$). The shape of the η–$\dot{\gamma}$ curve in the onset region agreed fairly well in most cases with a theoretical master curve for monodisperse polymers[23] (Figure 6–8). For consistency, and to smooth out experimental scatter, the data were superimposed on the master curve and values of $\dot{\gamma}_0$ were read off as those corresponding to η/η_0 = 0.8 on the master curve. In a few cases, where the shape did not agree with the master curve, primarily the

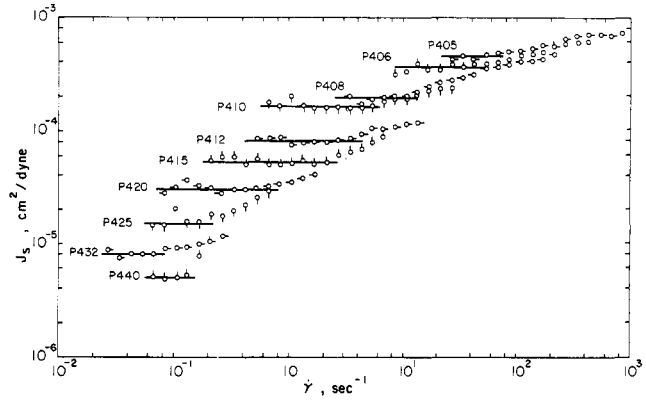

Figure 4. Normal stress compliance J_s vs. shear rate for linear polyisoprene at several concentrations. The sample is P4 ($\bar{M}_w$ = 1 611 000); the last two digits in the code indicate the approximate weight percentage of polymer in each solution.

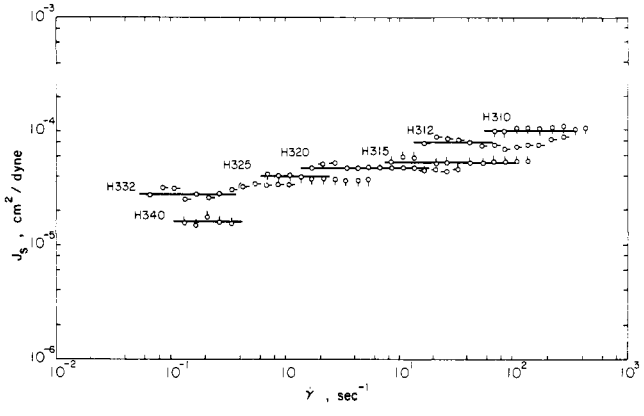

Figure 5. Normal stress compliance J_s vs. shear rate for six-arm polyisoprene at several concentrations. The sample is H3 ($\bar{M}_w$ = 1 446 000); the approximate weight percentage of polymer is given by the last two digits in the code.

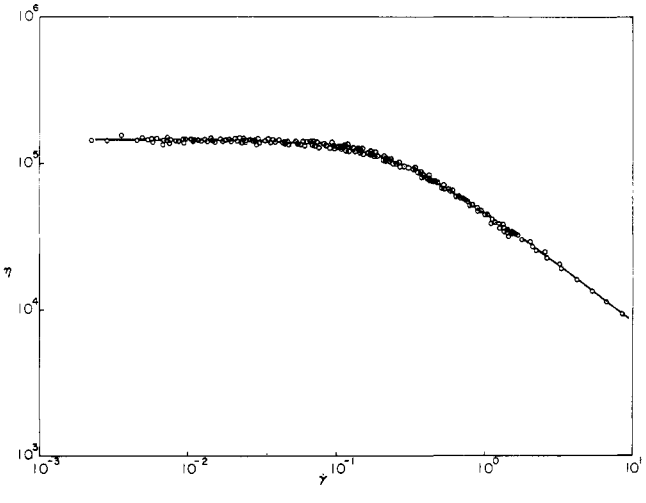

Figure 6. Viscosity–shear rate master curve for linear polyisoprene sample P4 ($\bar{M}_w$ = 1.611 × 10⁶). Data at all concentrations have been shifted to produce best superposition with P425 (c = 0.200 g/ml). The solid line is a theoretical master curve for monodisperse polymers,[23] shifted to produce the best superposition.

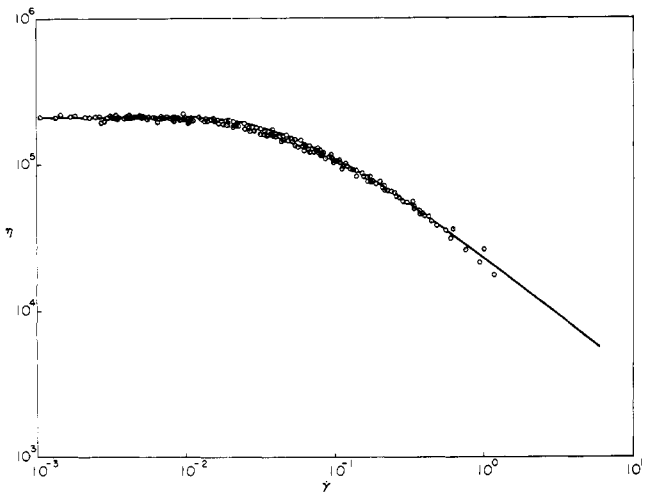

Figure 7. Viscosity–shear rate master curve for four-arm branched polyisoprene sample S6 ($\bar{M}_w = 1.95 \times 10^6$). Data at all concentrations have been shifted to produce best superposition with S625 (c = 0.198 g/ml). The solid line is the theoretical curve in Figure 6.

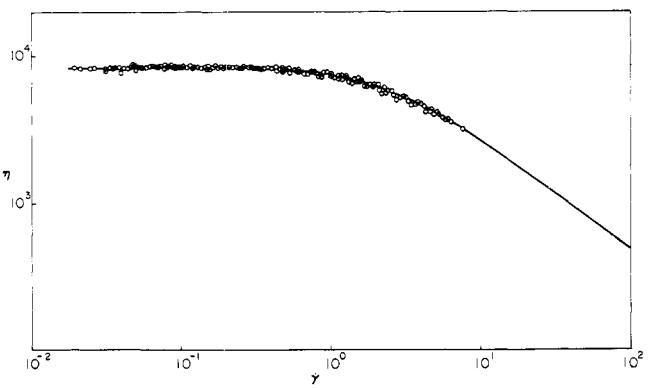

Figure 8. Viscosity–shear rate master curve for six-arm branched polyisoprene sample H3 ($\bar{M}_w = 1.446 \times 10^6$). Data at all concentrations have been shifted to produce best superposition with H325 (c = 0.203 g/ml). The solid line is the theoretical curve in Figure 6.

data on sample S6 at various concentrations, visual fits above and below the onset region were used to fix $\dot{\gamma}_0$. Values of $\dot{\gamma}_0$ obtained by these procedures are directly comparable with those used to obtain eq 18 for linear narrow distribution polymers.[10]

The normal stress difference became measurable only for shear rates approaching $\dot{\gamma}_0$ and beyond. Thus only a small region was available in which the limiting behavior, $N_1 \propto \dot{\gamma}^2$, was observed. For simple fluids,

$$\lim_{\dot{\gamma}\to 0} \frac{N_1}{\dot{\gamma}^2} = 2J_e^0\eta_0^2 \tag{19}$$

or

$$\lim_{\dot{\gamma}\to 0} \frac{N_1}{2\sigma^2} = J_e^0 \tag{20}$$

The quantity $J_s(\dot{\gamma}) \equiv N_1/2\sigma^2$ was found to vary only slowly with shear rate (Figures 2, 4, and 5). Values of J_e^0 were estimated for each sample from $J_s(\dot{\gamma})$ at low shear rates. Here, for reasons that are presently unclear, the behavior of branched samples differed appreciably from the linear samples in being seemingly more subject to experimental scatter. Duplicate runs agreed fairly well but always with more uncertainty in the branched samples.

Early development of the flow instability prevented a determination of N_1 in some low molecular weight samples.

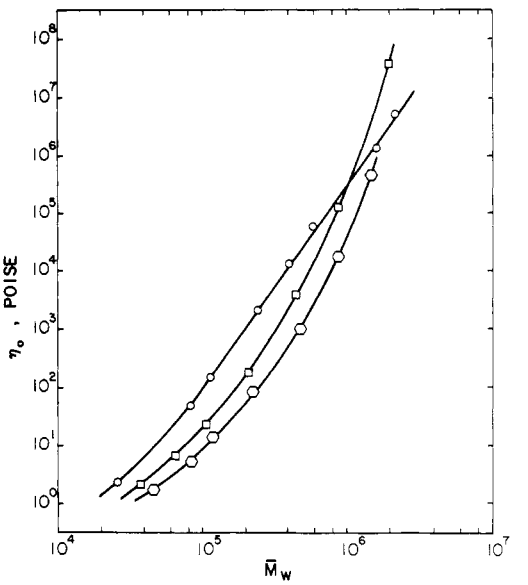

Figure 9. Zero-shear viscosity vs. molecular weight for linear and branched polyisoprenes at comparable concentration. The concentration in all cases is approximately 0.33 g/ml (see Table II): linear polymers (○), four-arm stars (□), and six-arm stars (⬡) are represented.

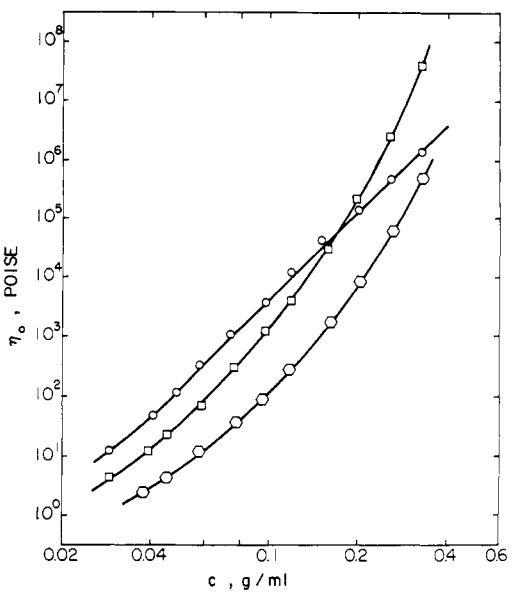

Figure 10. Zero-shear viscosity vs. concentration for linear and branched polyisoprenes of comparable molecular weight. The linear polymer (○) is sample P4 ($\bar{M}_w$ = 1 611 000); the four-arm star (□) is S6 ($\bar{M}_w$ = 1 950 000); the 6-arm star ( ) is H3 ($\bar{M}_w$ = 1 446 000).

The long time to reach steady state was a troublesome problem in the high molecular weight samples at high concentration. In the most extreme cases, the achievement of steady state in N_1 required 15 min at low shear rates. No difficulties with solvent evaporation or other changes in the samples occurred over the time span of the experiments, or even overnight at 25 °C. Indeed, even data obtained a few months apart with different aliquots of the same solution agreed very well.

Values of η_0, J_e^0, and $\dot{\gamma}_0$ for each solution are given in Table II.

III. Results

A. Zero-Shear Viscosity η_0. Figures 9 and 10 compare the molecular weight and concentration dependence of η_0

Table II
Summary of Rheological Parameters

Sample	$\bar{M}_w \times 10^{-3}$	c, g/cm^3	η_0, P	J_e^0, cm^2/dyn	$\dot{\gamma}_0$, s^{-1}
H5P40	25.7	0.326	2.33×10^0		
H2P40	83.0	0.328	5.05×10^1	3.7×10^{-6}	1.57×10^3
P140	115	0.327	1.55×10^2	4.2	6.4×10^2
S8P40	240	0.329	2.06×10^3	6.3	4.8×10^1
P540	394	0.328	1.25×10^4	4.6	8.8×10^0
P340	591	0.336	6.0×10^4	5.2	2.2×10^0
P440	1611	0.331	1.35×10^6	5.0	6.1×10^{-2}
P432		0.257	4.70×10^5	8.0	1.15×10^{-1}
P425		0.200	1.43	1.5×10^{-5}	1.79
P420		0.151	4.45×10^4	2.97	4.0
P415		0.120	1.21	5.2	8.4
P412		0.0979	3.82×10^3	8.0	1.63×10^0
P410		0.0742	1.12	1.60×10^{-4}	3.25
P408		0.0586	3.14×10^2	1.90	6.4
P406		0.0484	1.08	3.55	1.35×10^1
P405		0.0403	4.65×10^1	4.40	2.27
P404		0.0290	1.19	5.5	7.5
P240	2225	0.328	5.8×10^6	4.7×10^{-6}	1.63×10^{-2}
P215		0.152	3.00×10^4	6.2×10^{-5}	2.7×10^{-1}
S440	37.8	0.326	2.07×10^0		
S740	67.1	0.329	6.9		
S240	107.6	0.337	2.30×10^1	2.8×10^{-6}	
S140	215	0.330	1.85×10^2	8.0	2.37×10^2
S340	449	0.332	3.6×10^3	9.0	1.70×10^1
S840	880	0.326	1.25×10^5	1.46×10^{-5}	2.20×10^{-1}
S640	1950	0.326	$(3.8 \times 10^7)^a$	1.72	$(4.4 \times 10^{-4})^a$
S632		0.257	2.50×10^6	4.0	5.1×10^{-3}
S625		0.198	2.14×10^5	6.3	3.85×10^{-2}
S620		0.158	2.89×10^4	8.2	2.57×10^{-1}
S615		0.119	3.78×10^3	9.5	1.90×10^0
S612		0.0967	1.21	9.6	4.5×10^0
S610		0.0773	2.90×10^2	1.17×10^{-4}	1.22×10^1
S608		0.0587	7.3×10^1	1.61	3.35×10^1
S606		0.0449	2.22	2.20	7.5×10^1
S605		0.0394	1.23	2.60	1.22×10^2
S604		0.0291	4.2×10^0	2.8	3.2×10^2
H740	45.4	0.324	1.73		
H640	85.7	0.325	5.42		
H540	122	0.335	1.35×10^1	3.0×10^{-6}	
H140	226	0.340	8.1	3.8	9.0×10^2
H240	478	0.327	9.7×10^2	7.6	6.3×10^1
H440	870	0.330	1.76×10^4	1.20×10^{-5}	2.1×10^0
H340	1446	0.329	4.70×10^5	1.60	5.5×10^{-2}
H332		0.262	5.9×10^4	2.75	3.35×10^{-1}
H325		0.203	8.3×10^3	3.9	1.75×10^0
H320		0.161	1.67	4.65	8.0×10^0
H315		0.118	2.87×10^2	5.2	3.0×10^1
H312		0.0951	8.7×10^1	8.0	7.8
H310		0.0788	3.55	1.00×10^{-4}	1.50×10^2
H308		0.0579	1.18	9.8×10^{-5}	2.9
H306		0.0456	4.25×10^0	1.03×10^{-4}	6.4
H305		0.0377	2.33		9.5

[a] Separate values of η_0 and $\dot{\gamma}_0$ for S640 are somewhat uncertain because an unambiguous entry into the limiting region at low shear rates could not be made. However, the product $\dot{\gamma}_0\eta_0$ is less uncertain because the errors in η_0 and $\dot{\gamma}_0$ are compensatory.

for the three types of polymer structure. At high concentration but low molecular weight the viscosities of the branched samples are considerably less than those of linear samples of the same molecular weight. At high molecular weights the reverse becomes true, with branched polymers tending to show enhanced viscosities. However, as the concentration is reduced the enhancement disappears even at high molecular weights, and the viscosities of branched samples are again considerably less than those of corresponding linear samples. These results are qualitatively consistent with the observations of Kraus and Gruver on three-star and four-star polybutadienes[2b,19] and with the suggestions of those workers and Berry and Fox[2a] that the enhancement factor Γ_1 is highly sensitive to both concentration and branch length.

Data on the linear polymer solutions obey the empirical relationship:

$$\eta_0 = 0.86 \times 10^{-13} c^5 M^{3.5} \quad (21)$$

except at low molecular weights (Figure 11).

The intrinsic viscosity in tetradecane, $[\eta]_{TD}$, is proportional to $M^{0.679}$, and within experimental error the linear polymer correlation can just as well be expressed as (Figure 12):

$$\eta_0 = 6.3 \times 10^5 (c[\eta]_{TD})^5 \quad (22)$$

Thus, although $cM > \rho M_c$ for practically all solutions investigated, there is no reason on the basis of the data presented here to prefer the high concentration form (eq 21) than the low to moderate concentration form (eq 22) for evaluation of enhancement factor.

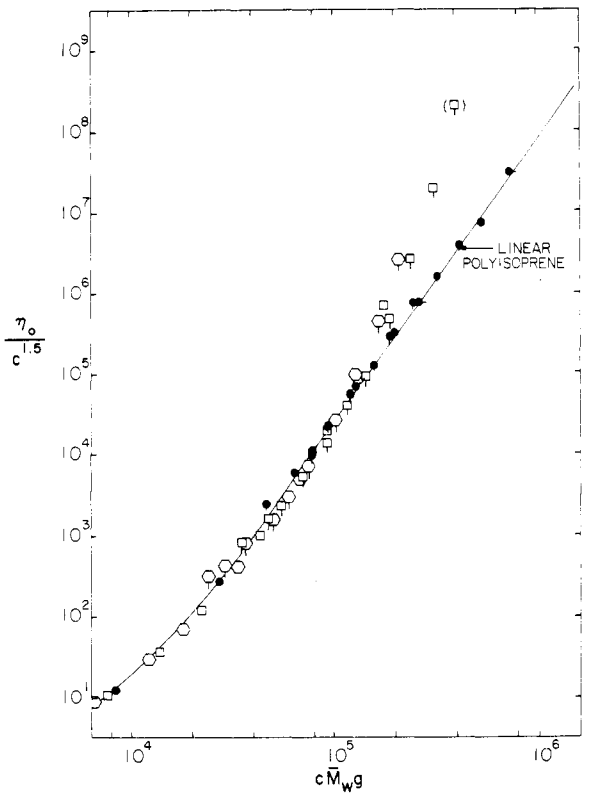

Figure 11. Comparison of zero-shear viscosity in linear and branched polyisoprenes through the reducing parameter $c\bar{M}_w g$. The symbols indicate various concentrations of S6 (⊡), the remaining four-arm stars at approximately c = 0.33 g/ml (□), various concentrations of H3 (⬡), and the remaining six-arm stars at approximately c = 0.33 g/ml (⬡). Data for the linear samples are indicated by small filled circles (●).

According to the earlier discussion, it might be hoped to reduce both branched and linear polymer data to the same correlating form in the absence of enhancement. Equation 22 is already a candidate for the unified correlation. Equation 21, from the standpoint of high concentration theory, reflects fully entangled behavior with a = 3.5 and a frictional coefficient proportional to $c^{1.5}$. Accordingly,

$$\eta_0 = 0.86 \times 10^{-13} c^{1.5} (cgM)^{3.5} \quad (23)$$

is also a candidate for a unified correlation in the absence of enhancement. Finally, with g replaced by $([\eta]_\theta)_B^2/([\eta]_\theta)_L^2$ (eq 8) and M expressed in terms of $([\eta]_\theta)_L$, eq 23 becomes

$$\eta_0 = 1.20 \times 10^7 c^{1.5} (c[\eta]_\theta^2)^{3.5} \quad (24)$$

presenting a third possibility for unified correlation.

Figures 11–13 show η_0 for the branched polymers plotted according to eq 22, 23, and 24. The g values used in Figure 11 are theoretical ones ($g(4)$ = 5/8, $g(6)$ = 4/9), calculated from eq 9, but experimental values based on light scattering in a theta solvent[9] ($g(4)$ = 0.65, $g(6)$ = 0.46)) give essentially the same correlation.

The lines indicate the locus of the linear polymer data in each case. It is clear that all three bring the branched and linear data fairly close together except at high concentrations and molecular weights. It is interesting that the $c[\eta]_{TD}$ correlation yields virtually a single curve for all branched polymer solutions, even in the enhancement region. However, the curve for branched polymers is somewhat below the linear curve at midrange. Superposition at midrange and below can only be achieved by arbitrarily reducing all values of $[\eta]_{TD}$ for the branched polymers by approximately 12%.

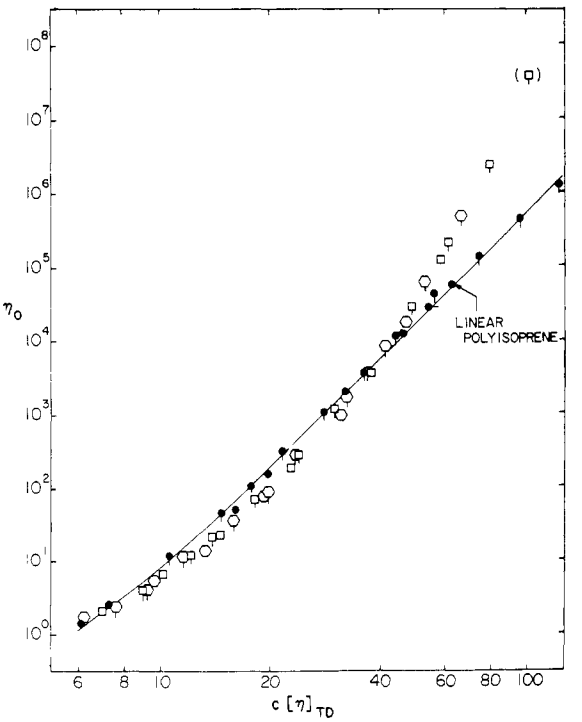

Figure 12. Comparison of zero-shear viscosity in linear and branched polyisoprenes through the reducing parameter $c[\eta]_{TD}$. The symbols are the same as in Figure 11.

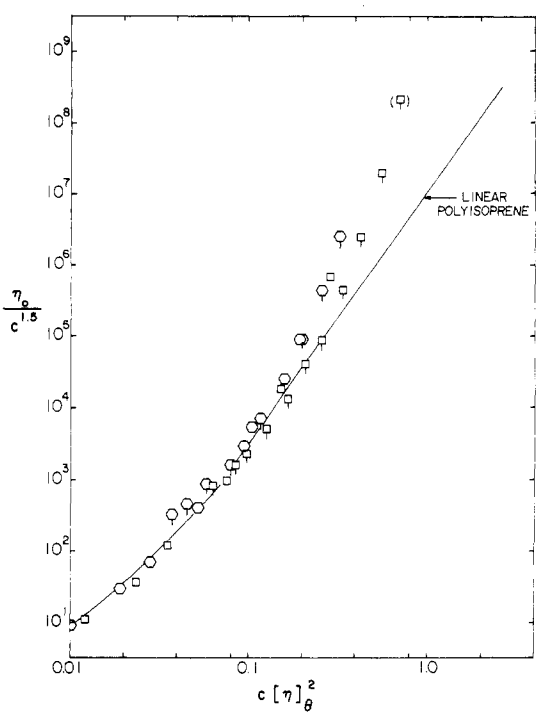

Figure 13. Comparison of zero-shear viscosity in linear and branched polyisoprenes through the reducing parameter $c[\eta]_\theta^2$. The symbols are the same as in Figure 11; the intrinsic viscosities are those measured in dioxane at 34 °C.

The correlations using the cgM and $c[\eta]_\theta^2$ variables give closer agreement between the branched and linear polymers at midrange and below. The enhancements here vary in different ways with concentration, molecular weight, and numbers of branches. Unification at midrange and below was comparable for both variables, so ratios $(\eta_0)_{obsd}/(\eta_0)_{calcd}$ were evaluated for each branched sample (c > 0.07 g/ml) using $(\eta_0)_{calcd}$ both from eq 23 and from eq 24. The

Table III
Summary of Enhancement Factors

Sample	$\bar{M}_w \times 10^{-3}$	c, g/cm³	Γ_1[a] Eq 23	Γ_1[a] Eq 24	Γ_2[b] Eq 28	Γ_2[b] Eq 15	Γ_3[c] Eq 34	$\Phi^{5/6}(\Phi M_b/M_c)$
S240	107.6	0.337	(1.00)	(1.40)	1.18	0.77		0.437
S140	215	0.330	1.01	0.98	2.29	2.11	2.51	0.842
S340	449	0.332	1.44	1.67	2.62	2.40	1.83	1.77
S840	880	0.326	5.26	6.55	4.06	3.75	3.92	3.35
S640	1950	0.326	(98.5)	(98.7)	4.79	4.42	6.25	7.44
S632		0.257	21.1	20.9	6.44	6.39	5.28	4.81
S625		0.198	6.80	6.40	5.58	5.97	4.82	2.97
S620		0.158	2.78	2.61	4.32	4.94	3.42	1.97
S615		0.119	1.49	1.37	2.60	3.25	2.00	1.17
S612		0.0967	1.35	1.22	1.63	2.16	1.75	0.800
S610		0.0767	1.00	0.90	1.19	1.69	1.72	0.523
S608		0.0587	1.00		0.88		1.43	0.320
H540	122	0.335	(1.00)	(1.33)	1.71	0.89		0.325
H140	226	0.340	1.00	0.90	1.28	1.16	1.77	0.621
H240	478	0.327	1.13	1.10	2.34	2.15	1.95	1.22
H440	870	0.330	2.39	2.44	3.79	3.46	3.30	2.26
H340	1446	0.329	11.0	11.1	5.02	4.60	4.68	3.73
H332		0.262	4.25	4.24	5.10	4.92	3.89	2.46
H325		0.203	2.15	2.08	4.02	4.24	3.18	1.54
H320		0.161	1.38	1.31	2.82	3.20	2.18	1.01
H315		0.118	1.00	1.03	1.53	1.92	1.80	0.570
H312		0.0951	(1.00)	(0.88)	1.44	1.92	1.42	0.384
H310		0.0788	(1.00)	(0.92)	1.17	1.64	1.31	0.272
H308		0.0579	(1.00)				1.10	

[a] Equation numbers refer to source of $(\eta_0)_{calcd}$. [b] Equation numbers refer to source of $(J_e^0)_{calcd}$. [c] Equation number refers to source of $(1/\eta_0\gamma_0)_{calcd}$.

ratios evaluated with eq 23 leveled off smoothly to values of approximately 0.61 at midrange and below for both four-arm and six-arm stars. The values of Γ_1 from eq 23 (Table III) were therefore calculated by dividing each ratio by 0.61. The ratios evaluated with eq 24 leveled off smoothly to approximately 0.66 at midrange and below for the four-arm stars and to approximately 1.0 for the six-arm stars. The values of Γ_1 from eq 24 (Table III) were therefore calculated by dividing the four-star ratios by 0.65; the six-arm ratios were used without modification. The values of Γ_1 yielded by the two methods are seen to be rather similar.

B. Steady State Compliance J_e^0. Figure 14 shows J_e^0 for the linear samples plotted in the form suggested by eq 12 and 13, namely $J_e^0(cRT/M)$ as a function of the product cM. Also included are results published by other workers for linear polyisoprene solutions and melts.[24-26] For unknown reasons, the latter data lie consistently above those reported here. Differences in polydispersity, differences in microstructure (the earlier samples have somewhat higher cis-1,4 contents than ours), or differences due to systematic errors in the techniques used to obtain J_e^0 may be involved.

Even the data reported here do not conform precisely to a single curve, contrary to the form indicated by eq 12 and 13. Values of J_e^0 at constant concentration (c = 0.33 g/ml) are essentially independent of molecular weight as required by eq 13, but the concentration dependence appears to be more complicated. Figure 15 shows the concentration dependence of J_e^0 for two linear samples. A line corresponding to c^{-2} dependence (from eq 13) has been drawn through the values at high concentration ($c > 0.25$ g/ml). Data on both samples at lower concentrations clearly lie above this line. A line simply drawn through all data for which $c > 0.07$ g/ml yields $J_e^0 \propto c^{-2.3}$. Judged by the appearance of Figure 15 (and data on $\dot{\gamma}_0$ to be discussed subsequently) we believe that $J_e^0 \propto c^{-2}$ is the form approached at high concentrations.

Based on this inverse square relationship and the compliance values of all linear samples at a concentration of 0.33 g/ml (average $J_e^0 = 4.8 \times 10^{-6}$ cm²/dyn), we can estimate the compliance at the limit of high molecular weight for undiluted linear polyisoprene of narrow molecular weight distribution:

$$(J_e^0)_\infty = \frac{c^2}{\rho^2} J_e^0(c) = 0.63 \times 10^{-6} \text{ cm}^2/\text{dyn} \qquad (25)$$

The characteristic molecular weight M_c', obtained using eq 13 with $\alpha = 0.4$ and the average value of J_e^0 at $c = 0.33$ g/ml, is

$$M_c' = \frac{c^2 RT}{0.4\rho} J_e^0(c) = 35\,000 \qquad (26)$$

These values of $(J_e^0)_\infty$ and M_c' are in slightly better agreement with observations in other narrow distribution polymers than those deduced[10] from the earlier data[24-26] ($(J_e^0)_\infty = 1.4 \times 10^{-6}$ cm²/dyn; $M_c' = 60\,000$). For example, the product $(J_e^0)_\infty G_N^0$ is a measure of the breadth of the terminal relaxation spectrum.[10] The plateau modulus G_N^0 is approximately 3.9×10^6 dyn/cm² for natural rubber,[11] giving $(J_0^0)_\infty G_N^0 = 2.4_6$ with the results of this study. This value is somewhat lower than values of 2.9–3.5 obtained in several other polymers, but in somewhat better agreement than the rather high value of 5.4_6 which was obtained from the earlier data.[10] If $J_e^0 \propto c^{-2.3}$ were used to calculate $(J_e^0)_\infty$, the $(J_e^0)_\infty G_N^0$ product would have assumed an even smaller value of 1.8. Likewise, the ratio of characteristic molecular weights M_c'/M_c (again using $M_c = 10\,000$ for polyisoprene) is 3.5 from the data reported here, which is considerably lower than the value of 6.0 from the earlier data but in reasonable accord with values of 2.3–4.2 obtained for several other polymers.[10]

The molecular weight and concentration dependence of J_e^0 for the branched samples is illustrated in Figure 16 and 17, together with lines representing the Rouse–Ham equations for each of the three structures. The reduction in compliance due to branching is evident at low concentrations. The molecular weight dependence shows also a clear trend toward reduction at lower molecular weights. How-

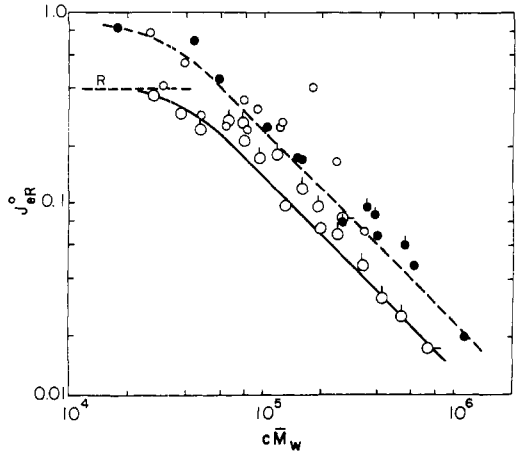

Figure 14. Reduced compliance as a function of $c\bar{M}_w$ for linear polyisoprene. The large open circles are data measured here for sample P2 (◯), sample P4 (◯), and the remaining samples (◯). The small circles are data obtained elsewhere[24–27] on solutions (○) and undiluted samples (●, ●).

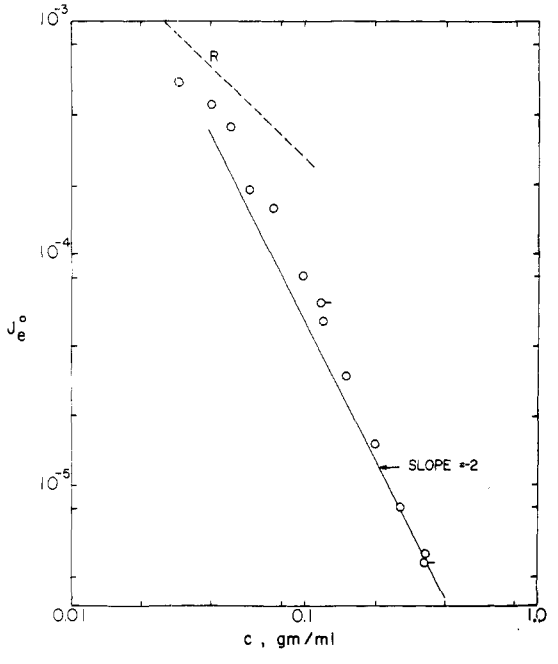

Figure 15. Recoverable compliance as a function of concentration for linear polyisoprene. The symbols indicate samples P4 (○) and P2 (○). The dashed line is the theoretical curve for sample P4 according to the Rouse model.

ever, at high concentrations and molecular weights the compliances of the branched polymers are consistently higher than their linear counterparts. The nature of the concentration dependence (Figure 17) is especially striking and unexpected, since the curves for both branched samples show inflections where they cross the curve for linear polymers. Similar and even more pronounced inflections are seen in the concentration dependence of $\dot{\gamma}_0$, discussed in the following section. No such inflections are evident in the molecular weight dependence (Figure 16). However, the data here are not as closely spaced and also more subject to scatter due to polydispersity differences among samples. Indeed, when the molecular weight dependence is examined by plotting J_e^0 vs. g_2M (Figure 18), the branched polymer behavior looks simply like a continuation of the behavior for low molecular weight linear samples, with the approach to a limiting compliance delayed until somewhat higher molecular weights are reached.

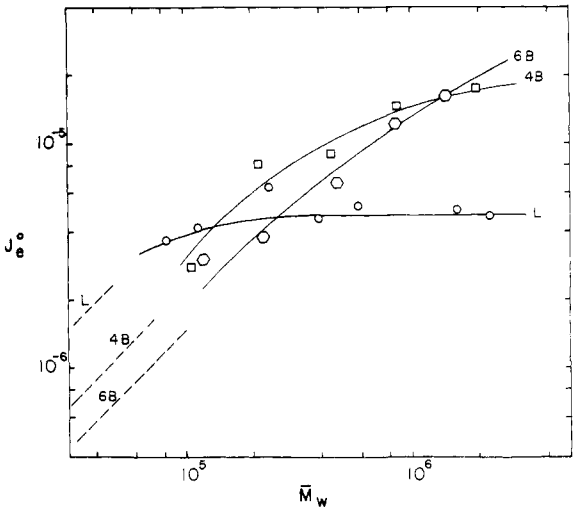

Figure 16. Recoverable compliance as a function of molecular weight for linear and branched polyisoprene. All concentrations are c = 0.33 g/ml; the symbols have the same meaning as in Figure 9. The dashed lines are calculated from the Rouse–Ham theory for c = 0.33 g/ml.

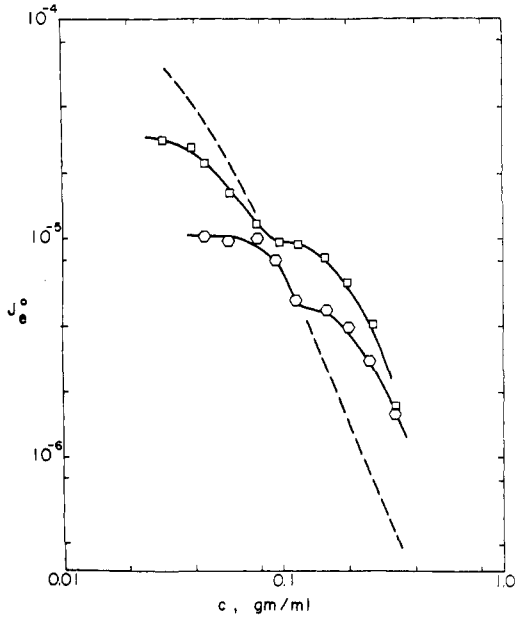

Figure 17. Recoverable compliance vs. concentration for branched samples of polyisoprene. The four-arm star (□) is sample S6 ($\bar{M}_w$ = 1 950 000); the six-arm star (○) is sample H3 ($\bar{M}_w$ = 1 446 000). The dashed line represents the data for the linear sample P4 ($\bar{M}_w$ = 1 611 000) shown in Figure 15.

The nonsimple behavior of J_e^0 in the linear polymers somewhat complicates the determination of compliance enhancement factors. Values of Γ_2 were determined in two ways, one through the use of eq 14 and 15 despite their imprecise fit to the data for linear samples, and the other with empirical equations which fit the linear results more or less faithfully at the higher concentrations ($c > 0.07$ g/ml):

$$(J_e^0)_{\text{calcd}} = 0.4g_2M/cRT \qquad (27)$$

$$cgM < 32\,000(0.33/c)^{0.3}$$

$$(J_e^0)_{\text{calcd}} = \frac{0.4g_2 32\,000(0.33/c)^{0.3}}{gc^2RT} \qquad (28)$$

$$cgM > 32\,000(0.33/c)^{0.3}$$

Values of Γ_2 by the former method were determined by plotting $J_e^0RT/0.4g_2M$ vs. $1/gc^2M$ (a rearranged version of

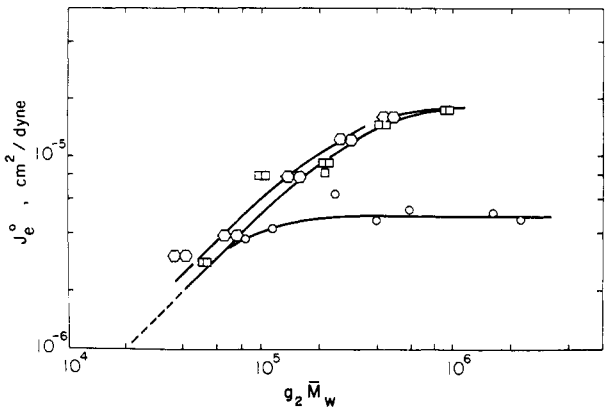

Figure 18. Recoverable compliance vs. $g_2\bar{M}_w$ for linear and branched polyisoprenes. The symbols have the same meaning as in Figure 9; the Rouse–Ham theory for c = 0.33 g/ml is indicated by the dashed line.

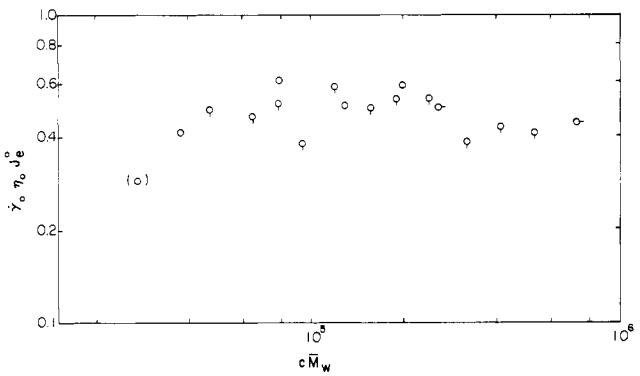

Figure 19. The product $\dot{\gamma}_0\eta_0 J_e^0$ vs. $c\bar{M}_w$ for linear polyisoprene. The symbols have the same meaning as in Figure 14.

eq 15) and evaluating $(J_e^0)_{calcd}$ for each branched sample from the locus of points defined by the linear samples. Values of Γ_2 by the latter method were determined from $(J_e^0)_{calcd}$, which were computed directly from eq 27 and 28. Theoretical values of g and g_2 were used in both cases. The differences in Γ_2 from the two methods are not large. The trend toward increased Γ_2 values with increasing concentration and molecular weight is apparent in Table III.

C. Characteristic Shear Rate $\dot{\gamma}_0$. The product $\dot{\gamma}_0\eta_0 J_e^0$ for the linear polymers is shown as a function of cM in Figure 19. No particular trend with either molecular weight or concentration is apparent. The mean and standard deviation of the values are

$$(\dot{\gamma}_0\eta_0 J_e^0)_{Linear} = 0.483 \pm 0.093 \quad (18 \text{ solutions}) \quad (29)$$

which falls within the range observed for other linear polymers.[10]

Figure 20 compares $\dot{\gamma}_0\eta_0 J_e^0$ for the branched polymers with the mean for the linear polymers. There may be some small systematic variation here, with perhaps a broad maximum at intermediate values of cM. However, the means and standard deviations are similar to those for the linear polymers:

$$(\dot{\gamma}_0\eta_0 J_e^0)_{4\text{-branch}} = 0.456 \pm 0.114 \quad (14 \text{ solutions}) \quad (30)$$

$$(\dot{\gamma}_0\eta_0 J_e^0)_{6\text{-branch}} = 0.458 \pm 0.115 \quad (12 \text{ solutions}) \quad (31)$$

Thus, if there are differences due to branching, they are not large.

The product $\eta_0\dot{\gamma}_0$ may be regarded as a kind of a characteristic shear stress σ_0, separating the Newtonian and power law regions. Branched systems which show enhanced

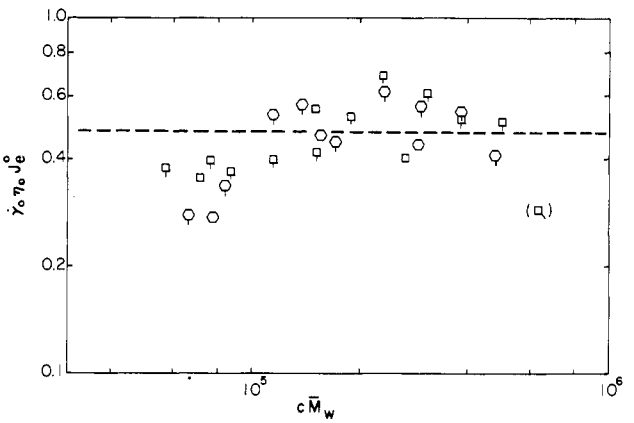

Figure 20. The product $\dot{\gamma}_0\eta_0 J_e^0$ vs. $c\bar{M}_w$ for branched polyisoprene. The dashed line is the mean value of the product for linear polyisoprene. The symbols have the same meaning as in Figure 11.

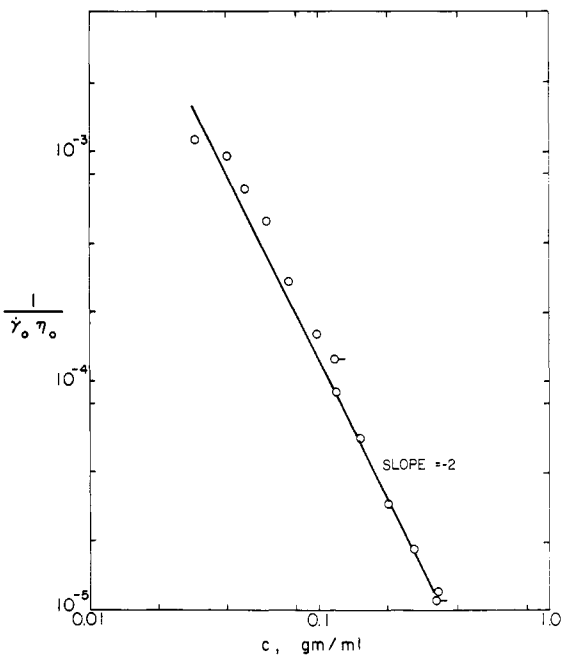

Figure 21. The quantity $1/\dot{\gamma}_0\eta_0$ vs. concentration for linear polyisoprene. The symbols have the same meaning as in Figure 15.

values of J_e^0 must therefore have reduced values of σ_0. Thus, shear rate dependence in the viscosity begins at lower steady state stresses in branched polymers with enhanced compliances than in comparable linear polymers.

The difficulties in estimating J_e^0 from the normal stress, particularly for branched samples, were noted earlier. Certain anomalies in the concentration dependence of J_e^0 for both the linear (Figure 15) and branched (Figure 17) samples were also pointed out. It is therefore worthwhile to examine the concentration dependence of the product $\dot{\gamma}_0\eta_0$ since its behavior is clearly related to J_e^0, and yet it is obtained from the shear stress measurement rather than the normal stress.

If the product $\dot{\gamma}_0\eta_0 J_e^0$ is taken to be literally constant, the concentration dependence of $1/\dot{\gamma}_0\eta_0$ should parallel that of J_e^0, and any peculiarities in J_e^0 vs. c should be reflected by $1/\dot{\gamma}_0\eta_0$ vs. c also. Figure 21 shows the behavior for linear polymers. Departures from c^{-2} dependence are present, but they are somewhat smaller than observed for J_e^0 (Figure 15). It also appears that c^{-2} dependence extends over a reasonable range at high concentrations. We take this as further justification of our earlier assumption

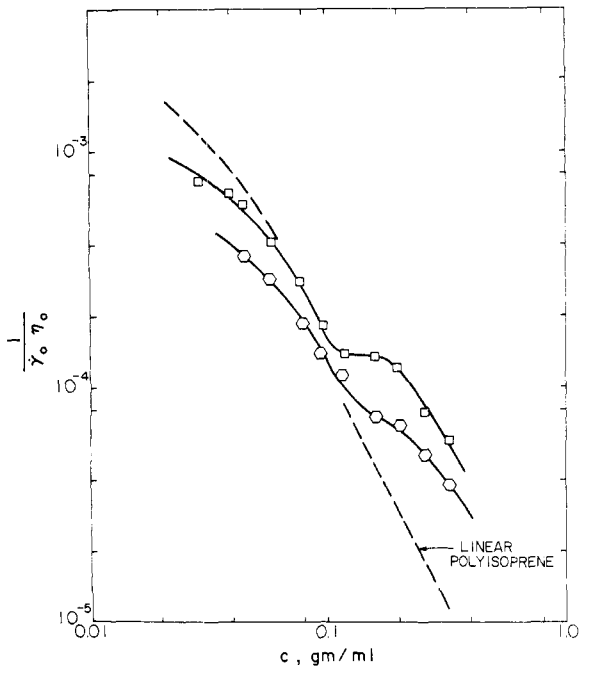

Figure 22. The quantity $1/\dot{\gamma}_0\eta_0$ vs. concentration for branched samples of polyisoprene. The symbols have the same meaning as in Figure 17. The dashed line represents the data for the linear sample P4 ($\bar{M}_w$ = 1 611 000) shown in Figure 21.

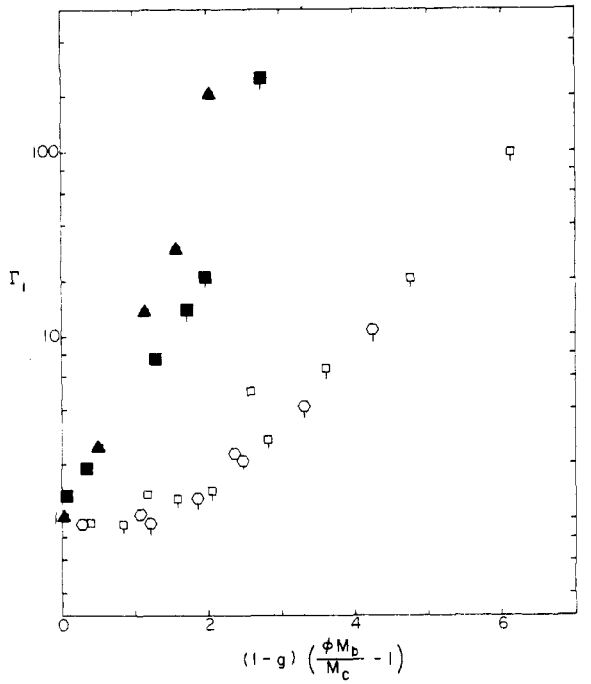

Figure 23. Viscosity enhancement in star-branched polyisoprene and polybutadiene plotted according to the Berry–Fox relation. Polyisoprene data are indicated by the open symbols, with the same meanings as in Figure 11. The polybutadiene data of Kraus and Gruver[2b,19] are indicated by filled symbols: undiluted three-arm stars (▲), the same four-arm star sample both in solution and undiluted (◆), and undiluted four-arm stars (■).

of c^{-2} behavior to estimate $(J_e^0)_\infty$ for undiluted polyisoprene. Figure 22 shows the concentration dependence of $1/\dot{\gamma}_0\eta_0$ for branched polymers. If anything, the inflections near the curve for linear polymers are even more pronounced than in J_e^0 vs. c (Figure 17). We conclude therefore that the inflections are real and not artifacts of some systematic error in estimating J_e^0 from the normal stress measurements.

An enhancement factor for $1/\dot{\gamma}_0\eta_0$ can be evaluated, following the procedures used for η_0 and J_e^0:

$$\Gamma_3 = (1/\dot{\gamma}_0\eta_0)_{obsd}/(1/\dot{\gamma}_0\eta_0)_{calcd} \tag{32}$$

Aside from a small systematic departure due to the anomalous concentration dependence, data on the linear samples were found to obey eq 12 and 13 fairly well with $1/\dot{\gamma}_0\eta_0$ in place of J_e^0 and α taken to be 1.03. Thus, $(1/\dot{\gamma}_0\eta_0)_{calcd}$ was evaluated for branched samples from equations paralleling eq 14 and 15:

$$1/\dot{\gamma}_0\eta_0 = 1.03 g_2 M/cRT \qquad cgM < \rho M_c' \tag{33}$$

$$1/\dot{\gamma}_0\eta_0 = 1.03 \frac{g_2 M}{cRT}\left(\frac{\rho M_c'}{cgM}\right) \qquad cgM > \rho M_c' \tag{34}$$

Values of Γ_3 so obtained are given in Table III. They are of course similar in magnitude to the corresponding values of Γ_2. They will be discussed together with Γ_1 and Γ_2 in the following section.

IV. Discussion

A. Enhancement of Viscosity. Berry and Fox[2a] have suggested an empirical expression for the enhancement factor Γ_1 in undiluted polymers. For f-arm stars their equation reduces to

$$\ln \Gamma_1 = 2.16(1-g)\left[\frac{M}{fM_c} - 1\right] \qquad M_b > M_c$$
$$\ln \Gamma_1 = 0 \qquad M_b < M_c \tag{35}$$

The natural generalization for highly concentrated solutions is

$$\ln \Gamma_1 = 2.16(1-g)\left[\frac{cM}{f\rho M_c} - 1\right] \qquad cM > f\rho M_c$$
$$\ln \Gamma_1 = 0 \qquad cM < f\rho M_c \tag{36}$$

Figure 23 shows the experimental values of Γ_1 plotted according to this expression, with M_c taken to be 10 000 for linear polyisoprene and c/ρ equal to the volume fraction of polymer Φ. On the same figure are the data of Kraus and Gruver on three-star and four-star polybutadienes (M_c = 5900), both undiluted[19] and in concentrated solutions.[2] Viewed in this way, there are clearly some rather sizable differences in enhancement magnitude between the two polymers, and smaller but nevertheless discernable differences among the various samples of each.

Other published data for equal-arm stars in which the linear polymer rheology is well established are those on undiluted four-arm polystyrene[5] (M_c = 33 000) and solutions of four- and six-arm polystyrene in diethylbenzene.[8] According to eq 24 the concentrations were too low to produce enhancement in the Utracki–Roovers study,[8] and indeed those data correlated very well in terms of the reduction in size alone. On the other hand, viscosity enhancement should have been observable in the highest molecular weight samples used by Onogi and coworkers[5] ($\bar{M}_w \approx$ 600 000). In fact, very little enhancement, if any, was found, so eq 23 and 24 seem unfortunately to be of somewhat limited generality.

In summary, the viscosity data presented here show enhancements due to branching which are qualitatively similar to those of polybutadiene and poly(vinyl acetate).[2a] That is, the viscosity begins to exceed the viscosity for linear chains of the same radius when the branches themselves are long enough to be involved in several entanglements $\Phi M_b/M_c > 1$, Φ being the volume fraction of polymer c/ρ. The magnitude of enhancement differs however between star-branched polybutadiene and polyisoprene at

the same entanglement density. Moreover, even among branched polyisoprenes with the same number of arms, the molecular weight and concentration dependences of enhancement are somewhat different. The combined variable $\Phi M_b'/M_c$ is insufficient for correlation because enhancement grows more rapidly with volume fraction Φ at constant branch length M_b than with branch length at constant volume fraction.

The conventional ways of looking at entanglement effects in linear chains appear inadequate for explaining an additional enhancement due to branching. Bueche[14] and Graessley[23] visualize a resistance to flow in entangled linear chains as that arising from the additional systematic motions required of chains in order to pass around obstacles in their environs, such as the backbone contours of neighboring chains, rather than diffusing through them as a particle cloud. One could extend this picture to branched chains by postulating that, for sufficiently complex branched molecules, the entanglements involving portions of the molecules between branching nodes might present unusually high resistances, since the passage of a branching node around such an internal strand would likely require a much greater degree of cooperativity than in the case of an unbranched chain.

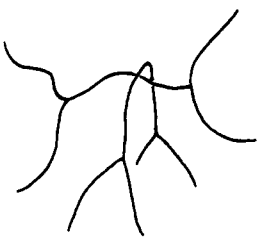

However, star molecules contain only one node, so slippage in this case need involve only extra motions for linear strands (the arms).

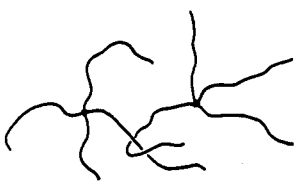

One would therefore expect very little enhancement in star molecules, or at least a substantially smaller effect in stars than combs, since only the latter have more than one node. However, enhancement seems roughly similar for both types of structure when compared at the same entanglement density for the branches.[2a] Thus, reasoning based on a simple slippage process must be in error.

DeGennes[28] has examined theoretically the diffusion of flexible random coils in a medium filled with loop-like obstacles. The chain is hemmed in by the obstacles, so to speak, which define a kind of tunnel along the chain contour. Diffusion is imagined to take place by a series of random, inching displacements along the tunnel, called reptation. As the chain diffuses out of its tunnel, established by its contour configuration at some initial time, it continually creates a new tunnel and thereby acquires a new configuration, defined by the path it happens to choose as it moves among the surrounding obstacles.

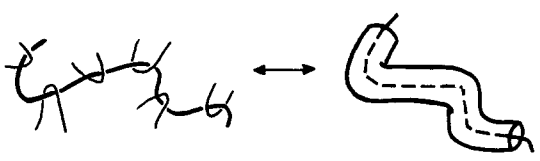

The configuration renewal time, or configurational relaxation time, is therefore of the order of the average time required for the chain to create an entirely new tunnel for itself by reptating diffusion. The picture is meant to apply to a permanent network and to the motion of a chain permeating but not connected to the network. Edwards and Grant[29] suggest in fact that in entangled systems without cross-links one really should consider the cooperative diffusion of chain and tunnel. Indeed, in nonentangled systems, tunnel diffusion becomes nothing more than diffusion of the entire chain as a particle cloud, the situation in dilute solutions.

Leaving aside any detailed considerations for the moment, it seems clear that the presence of long branches must drastically reduce the translational diffusion coefficient in reptating chains.

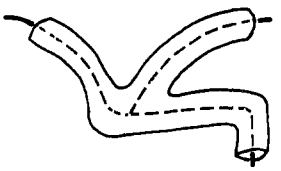

The reptating motion that allows a net translation of linear chains along an entanglement tunnel would seem to be rendered essentially ineffective by even one sufficiently long branch, and the translational diffusion coefficient of the center of gravity should be correspondingly reduced. To be sure, allowing the tunnel itself to diffuse in entangled but not cross-linked systems would provide some additional mobility. However, if the tunnel were itself composed of chains with immobilizing branches, then it seems likely that even the tunnel mobility would be small. Hence, compared to linear molecules, the net translational mobility of branched molecules in an environment of other branched molecules will be greatly reduced, and, by inference, the macroscopic viscosity will be correspondingly increased.[31]

In summary, taking a viewpoint which combines the reptating chain[28] and diffusing tunnel[29] suggestions, we can begin to understand qualitatively a reduction in large-scale molecular mobility, and presumably a corresponding increase in macroscopic viscosity, caused by long branches in entangled systems. Even one branching node in a molecule, if at least three of the strands emanating from it are long enough to entangle, would obviate or at least greatly reduce the efficiency of one translation mechanism always available to a linear chain, namely diffusion along its own contour. If the molecules surrounding a branched molecule are linear, i.e., if the system contains only a relatively low concentration of branched molecules, then a net translation might still occur, but at a somewhat reduced rate, by tunnel diffusion. On the other hand, if most molecules are branched, then even tunnel diffusion would be inhibited and translational mobility reduced still further.

These comments are not meant to imply that η_0 should approach infinity at some finite branch length or entanglement density. Paths for translation, however tortuous, must of course always be available in the absence of a permanent network structure. However, if branched chains are denied a large portion of the translation paths available to entangled linear chains (the latter already displaying a greatly reduced mobility), then relaxation time and zero-shear viscosity could easily attain levels which are too large to measure by the usual methods.

We noted earlier that the entanglement density of the branch, characterized by $\Phi M_b/M_c$, was insufficient for correlating both concentration and chain length effects on the viscosity enhancement Γ_1. However, the modified product

$(\Phi M_b/M_c)\Phi^{5/6}$ seems not only to unify the Γ_1 data on four-branch polyisoprene, but also to bring these data into somewhat better accord with the Kraus–Gruver data on branched polybutadiene. We were led to the additional $\Phi^{5/6}$ factor by an analogy with ordinary diffusion and the conjecture that enhancement depends on the geometry of the side tunnel alone. We assume in the following discussion that the molecular weight between entanglements is the same for linear and branched chains at the same total polymer concentration, i.e., that the plateau modulus G_N^0 is the same for branched and linear chains.

The rate of diffusion at steady state through a long tube is proportional to A/L, A being the cross-sectional area of the tube and L its length. Suppose the translation of a branched molecule proceeds by a sequence of small displacements of its center of gravity, involving for each displacement the diffusion of the branches into entirely new side tunnels. Suppose further that, besides the many variables which affect diffusion of linear and branched molecules similarly, the translation rate of branched molecules will depend also on the geometrical factor A/L of the side tunnel.

The tunnel cross section depends on the total concentration of entanglements in the system. The average number of entanglement points per molecule in a monodisperse system is $M/(M_e)_{soln} = \Phi M/M_e$, in which M_e is the molecular weight between entanglements in the undiluted polymer. The number of entanglement junctions per unit volume is therefore $1/2(cN_a/M)(\Phi M/M_e) = \rho\Phi^2 N_a/2M_e$, in which N_a is Avagadro's number. The average distance in space between entanglements is then $(2M_e/\rho\Phi^2 N_a)^{1/3}$, so the cross-sectional area of the tunnel, defined by the spatial density of entanglement junctions, is of the order of

$$A = (2M_e/\rho\Phi^2 N_a)^{2/3} \tag{37}$$

The effective tunnel length depends on the number of entanglements along the branch, which is $E_b = \Phi M_b/M_e$. The average distance between successive entanglement points R_e is simply the root-mean-square end-to-end distance of a linear strand with molecular weight $(M_e)_{soln}$ or $(R^2/M)^{1/2}(M_e/\Phi)^{1/2}$, in which R^2/M is the characteristic ratio for linear chains of the polymer in question. The effective tunnel length, or total path leading around E_b junction points, is then

$$L = E_b R_e = \left(\frac{\Phi M_b}{M_e}\right)\left(\frac{R^2}{M}\right)^{1/2}\left(\frac{M_e}{\Phi}\right)^{1/2} \tag{38}$$

The ratio L/A will be called the side tunnel impedence V. With R^2 replaced by $6S^2$ for random coils, the expression for V becomes

$$V = \left(\frac{\Phi M_b}{M_e}\right)\left(\frac{\Phi^{5/6}6^{1/2}\rho^{2/3}N_a^{2/3}(S^2/M)^{1/2}}{2^{2/3}M_e^{1/6}}\right) \tag{39}$$

From this, the nondimensional correlating variable $(\Phi M_b/M_c)\Phi^{5/6}$ may be extracted, leaving, aside from numerical factors of order unity, a specific topological impedence Z for side tunnels

$$Z = \frac{\rho^{2/3}N_a^{2/3}(S^2/M)^{1/2}(M_c/M_e)^{7/6}}{M_c^{1/6}} \tag{40}$$

and

$$V = Z\Phi^{5/6}\left(\frac{\Phi M_b}{M_c}\right) \tag{41}$$

Values of Z, calculated from the data in Table I of ref 2a, and with $M_c/M_e = 2$,[10] are given in Table IV for several common polymers.

Table IV
Specific Topological Impedences for Branch Points in Various Polymers

Polymer	M_c	Z, Å^{-1}
Polystyrene	32 000	0.0780
Poly(vinyl acetate)	24 500	0.0794
Polyisoprene	10 000	0.103
Polybutadiene	5 900	0.128
Polyethylene	3 800	0.143

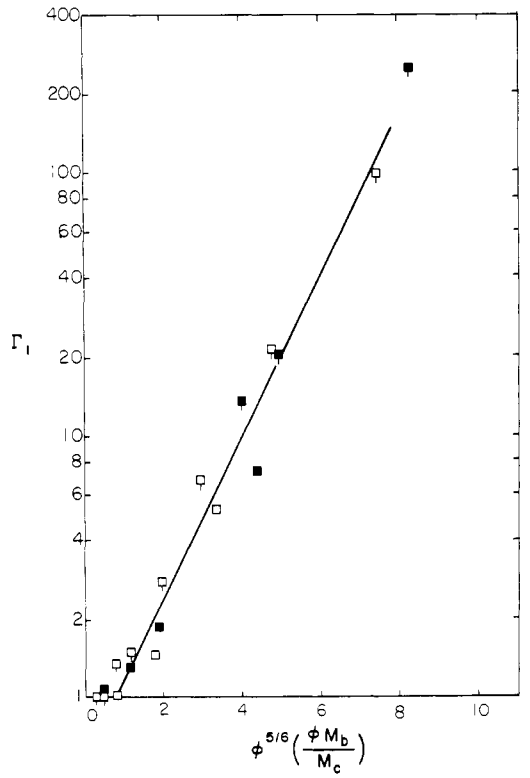

Figure 24. Viscosity enhancement in four-arm star polyisoprene and polybutadiene as a function of the tunnel parameter. The meaning of the symbols is the same as in Figure 23.

Figure 24 shows Γ_1 for four-branch polyisoprene and polybutadiene as a function of $(\Phi M_b/M_c)\Phi^{5/6}$. The agreement between the two polymers is remarkably good. However, if one accepts the values of Z in Table IV, and plots Γ_1 vs. V, the results for polybutadiene would lie slightly to the right of those for polyisoprene. Also, a detailed examination of the behavior for both polyisoprene and polybutadiene suggests that the $\Phi^{5/6}$ factor confers too strong a dependence on concentration. If $\Phi^{5/6}$ is replaced by $\Phi^{1/2}$ and Γ_1 is plotted as a function of $Z\Phi^{1/2}(\Phi M_b/M_c)$, the concentration and molecular weight dependences for each polymer are in somewhat better accord, and the agreement between polyisoprene and polybutadiene still remains quite good.

Figure 25 shows Γ_1 as a function of $(\Phi M_b/M_c)\Phi^{5/6}$ for three-branch polybutadiene and six-branch polyisoprene with a line indicating the locus of data on the four-branch polymers from Figure 24. The dependence on branching frequency is roughly as might be expected from the previous discussion, namely that the major contribution occurs with three-branch stars. The effect of additional branches progressively diminishes, with finally relative little effect on going from four-stars to six-stars. Comparisons in terms of the variable $Z\Phi^{1/2}(\Phi M_b/M_c)$ lead to the same conclusions. Finally, we note again that polystyrene stars do not

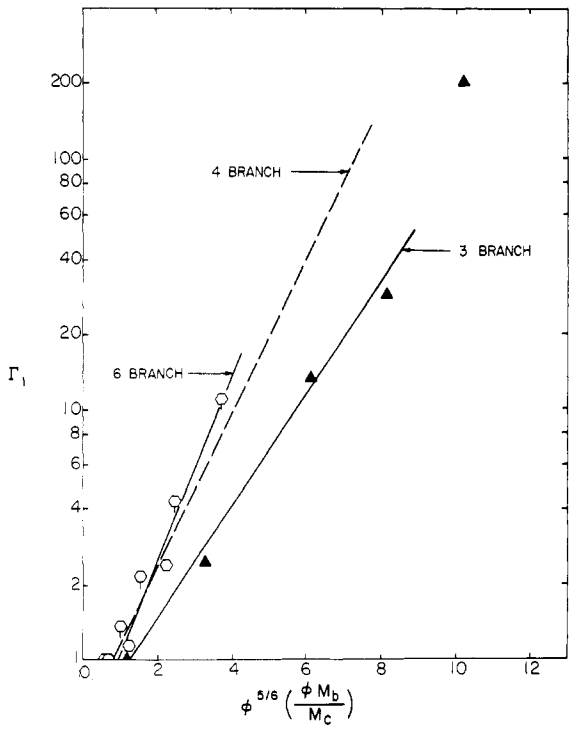

Figure 25. Viscosity enhancement in star polyisoprenes and polybutadienes with different numbers of arms. The meaning of the symbols is the same as it is in Figure 23.

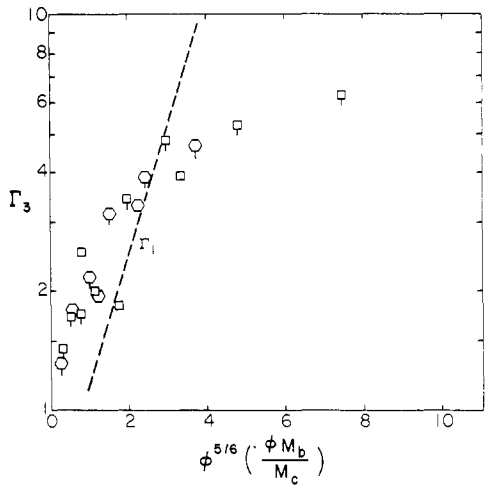

Figure 26. Enhancement of $1/\dot{\gamma}_0\eta_0$ in branched polyisoprenes. The symbols are the same as in Figure 11. The dashed line is the viscosity enhancement for four-arm and six-arm polyisoprenes as in Figure 25.

show viscosity enhancements in the same range of $\Phi^{5/6}(\Phi M_b/M_c)$ values as polyisoprene and polybutadiene. This behavior may stem from the unusually small specific topological impedence Z for polystyrene (Table IV), requiring somewhat larger entanglement densities to produce enhancement.

B. Enhancement of Compliance and Characteristic Time Constant. Figures 26 and 27 show Γ_3 and Γ_2 respectively as functions of $\Phi^{5/6}(\Phi M_b/M_c)$ for polyisoprene. As in the case of Γ_1, the differences between four-star and six-star samples are small. Also a somewhat better reduction of concentration and molecular weight dependences to a single curve would probably be obtained with $\Phi^{1/2}(\Phi M_b/M_c)$, as the independent variable. The experimental scatter is smaller in the case of Γ_3, which also shows a monotonic in-

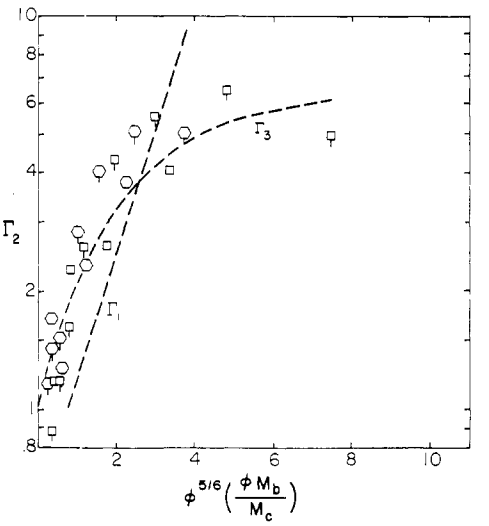

Figure 27. Enhancement in J_e^0 in branched polyisoprenes. The symbols are the same as in Figure 11. The corresponding enhancements in viscosity and $1/\dot{\gamma}_0\eta_0$ for four-arm and six-arm polyisoprenes are indicated by the dashed lines.

crease with concentration and molecular weight. The apparent maximum in Γ_2 may possibly indicate an underestimation of J_e^0 in the branched samples of highest concentration and molecular weight. The initial rise in both Γ_2 and Γ_3 begins at smaller values of $\Phi^{5/6}(\Phi M_b/M_c)$ and is relatively more abrupt than in the case of Γ_1. However, the values finally increase much less rapidly than Γ_1, suggesting perhaps the approach to some limiting value. It is interesting that the prominent inflections in the concentration dependence of J_e^0 and $1/\eta_0\gamma_0$ for the branched polymers (Figures 17 and 22) are not at all apparent in the Γ_2 and Γ_3 behavior; both depend smoothly on the parameter $\Phi^{5/6}(\Phi M_b/M_c)$.

In highly entangled polymers the viscosity η_0, steady-state compliance J_e^0, and plateau modulus G_N^0 are related to the number-and-weight average relaxation times of the terminal (post-plateau) relaxation spectrum $H(\tau)$:[10]

$$\eta_0/G_N^0 = \frac{\int_{-\infty}^{\infty} \tau H(\tau)\, d\ln\tau}{\int_{-\infty}^{\infty} H(\tau)\, d\ln\tau} \equiv \langle\tau\rangle_n \tag{42}$$

$$\eta_0 J_e^0 = \frac{\int_{-\infty}^{\infty} \tau^2 H(\tau)\, d\ln\tau}{\int_{-\infty}^{\infty} \tau H(\tau)\, d\ln\tau} \equiv \langle\tau\rangle_w \tag{43}$$

and

$$J_e^0 G_N^0 = \langle\tau\rangle_w/\langle\tau\rangle_n \tag{44}$$

Measurements on linear and branched polystyrenes indicate that G_N^0 is practically unaffected by branching.[5] Thus, the mean relaxation time and relaxation time dispersity of branched polymers in the terminal region, relative to linear polymers of the same molecular weight and concentration, can be expressed in terms of the enhancement factors

$$(\langle\tau\rangle_n)_{branched} = \Gamma_1 g^{3.5}(\langle\tau\rangle_n)_{linear} \tag{45}$$

$$(\langle\tau\rangle_w/\langle\tau\rangle_n)_{branched} = \Gamma_2 g_2(\langle\tau\rangle_w/\langle\tau\rangle_n)_{linear} \tag{46}$$

Enhancement of viscosity thus corresponds to an increase in the mean relaxation time of the terminal spectrum, while enhancement in compliance corresponds to a broadening of the terminal spectrum.

Attempts were made to relate Γ_1 and Γ_2 by postulating that a new set of relaxations at long times are generated by the presence of branching, and then searching for a suitable mixing rule (analogous to the treatment of the effects of molecular weight distribution[11] on η_0 and J_e^0). These attempts were unsuccessful; we never found it possible to predict the observed rapid rise in J_e^0 prior to or simultaneous with the rise in η_0. We conclude tentatively that the terminal spectrum broadens and shifts to longer times more or less simultaneously, and that the behavior cannot be explained simply by the development of a separate population of long-time relaxations alone. Finally, the results on branched polystyrenes,[3,5] showing large values of Γ_2 while Γ_1 remains near unity, suggest that viscosity and compliance enhancements need not always appear in the same relationship with one another. This characteristic and indeed the apparently unpredictable effects of branching on the temperature coefficient of viscosity[30] imply a disconcerting individuality among polymers in their response to branching.

The effect of branching on shear-rate dependence of viscosity deserves further comment. When Γ_3 is large, the onset of shear rate dependence is displaced to lower shear rates, compared to the behavior of linear polymers of the same molecular weight, or even of the same zero-shear viscosity. On the other hand, the results here and the data of Kraus and Gruver on polybutadiene[2b,19] suggest that the form of the viscosity master curve is not much affected by branching. A family of η–$\dot{\gamma}$ curves for narrow distribution linear polymers of various molecular weights tend to merge into a single curve at high shear rates.[10] The η–$\dot{\gamma}$ behavior at high shear rates for a branched polymer in the enhancement region will lie below this curve. Thus, a branched polymer in the enhancement region will display a higher viscosity at low shear rates than a linear polymer with the same radius of gyration, but will cross the linear η–$\dot{\gamma}$ curve at intermediate shear rates and then continue to remain below the linear curve at high shear rates. Indications of such behavior can be seen in Figure 4.

Acknowledgment. The authors are grateful to the U.S. National Science Foundation for the grant (GK 34362) supporting the rheological work.

References and Notes

(1) (a) Northwestern University; (b) National Research Council of Canada; (c) NRCC Postdoctoral Fellow 1972–1973.
(2) (a) G. C. Berry and T. G. Fox, *Adv. Polym. Sci.*, **5**, 261 (1968); (b) G. Kraus and J. T. Gruver, *J. Polym. Sci., Part A-2*, **8**, 305 (1970).
(3) T. Fujimoto, H. Narukawa, and M. Nagasawa, *Macromolecules*, **3**, 57 (1970).
(4) R. A. Mendelson, W. A. Bowles, and F. L. Finger, *J. Polym. Sci., Part A-2*, **8**, 105 (1970); *ibid.*, **8**, 127 (1970).
(5) T. Masuda, Y. Ohta, and S. Onogi, *Macromolecules*, **4**, 763 (1971).
(6) T. Masuda, Y. Nakagawa, Y. Ohta, and S. Onogi, *Polym. J.*, **3**, 92 (1972).
(7) J. Pannell, *Polymer*, **13**, 1 (1972).
(8) L. A. Utracki and J. E. L. Roovers, *Macromolecules*, **6**, 366 (1973); *ibid.*, **6**, 373 (1973).
(9) N. Hadjichristidis and J. E. L. Roovers, *J. Polym. Sci., Polym. Phys. Ed.*, **12**, 2521 (1974).
(10) W. W. Graessley, *Adv. Polym. Sci.*, **16**, 1 (1974).
(11) J. D. Ferry, "Viscoelastic Properties of Polymers", 2nd ed, Wiley, New York, N.Y., 1970.
(12) J. Brandrup and E. H. Immergut, Ed., "Polymer Handbook", Interscience, New York, N.Y., 1966.
(13) J. S. Ham, *J. Chem. Phys.*, **26**, 625 (1957).
(14) F. Bueche, *J. Chem. Phys.*, **40**, 484 (1964).
(15) B. H. Zimm and R. W. Kilb, *J. Polym. Sci.*, **37**, 19 (1959).
(16) P. E. Rouse, Jr., *J. Chem. Phys.*, **21**, 1272 (1953).
(17) K. Osaki, Y. Mitsuda, R. M. Johnson, J. L. Schrag, and J. D. Ferry, *Macromolecules*, **5**, 17 (1972).
(18) H. Leaderman, R. G Smith, and L. C. Williams, *J. Polym. Sci.*, **36**, 233 (1959).
(19) G. Kraus and J. T. Gruver, *J. Polym. Sci., Part A*, 105 (1965).
(20) W. W. Graessley, R. L. Hazleton, and L. R. Lindeman, *Trans. Soc. Rheol.*, **11**, 267 (1967).
(21) W. W. Graessley and L. Segal, *Macromolecules*, **2**, 49 (1969).
(22) W. C. Uy and W. W. Graessley, *Macromolecules*, **4**, 458 (1971).
(23) W. W. Graessley, *J. Chem. Phys.*, **47**, 1942 (1967).
(24) N. Nemoto, M. Moriwaki, H. Odani, and M. Kurata, *Macromolecules*, **4**, 215 (1971).
(25) N. Nemoto, H. Odani, and M. Kurata, *Macromolecules*, **5**, 531 (1972).
(26) N. Nemoto, T. Ogawa, H. Odani, and M. Kurata, *Macromolecules*, **5**, 641 (1972).
(27) G. V. Vinogradov, A. Ya. Malkin, Yu G. Yanovskii, E. K. Borisenkova, B. V. Yarlykov, and G. V. Berezhnaya, *J. Polym. Sci., Part A-2*, **10**, 1061 (1972).
(28) P. G. DeGennes, *J. Chem. Phys.*, **55**, 572 (1971).
(29) S. F. Edwards and J. W. V. Grant, *J. Phys. A: Math. Nucl. Gen.*, **6**, 1169 (1973).
(30) W. W. Graessley and E. S. Shinbach, *J. Polym. Sci.*, **12**, 2047 (1974).
(31) A preprint received from Dr. DeGennes at the time this article was being readied for publication describes very similar conclusions regarding the effect of branching on molecular mobility. He finds in addition that mobility should be an exponentially decreasing function of branch length in reptating systems, a result which accounts for the form of Γ_1 found experimentally (eq 36) when expressed in terms of macroscopic viscosity.